振動을 利用한 뿌리作物收穫機의 所要動力 및 土壤破碎에 關한 硏究(I)

—힘의 平衡 및 토크分析—

Effects of an Oscillating Inclined Blade on Soil Break-up and Energy Requirements(I).

—Balancing and Torque Analysis—

姜 和 錫*, 맬콤 라이트**, 鄭 昌 柱***, 金 相 憲*

W. S. Kang, Malcolm E. Wright, C. J. Chung, S. H. Kim

摘 要

뿌리作物을 收護하기 爲하여 振動을 利用한 4節링크로 構成되는 試作機를 設計, 製作 및 實驗을 遂行하였다. 收護機의 作動中 發生하는 不均衡力을 相殺시키기 爲한 힘의 平衡裝置를 設計하기 爲하여 各 要素의 加速度 및 動力學的인 힘을 分析하였고, 振動機構에 依하여 發生되는 理論的인 토크와 測定된 토크를 比較分析하였다. 設計된 힘의 平衡裝置는 不均衡力의 大部分을 相殺시켜주고, 理論的인 토크는 實測토크의 變化傾向과 잘 一致하였다.

I. INTRODUCTION

Moldboard plows, subsoilers and other non-vibrating tillage tools used in root-crop harvesting require large tractors to produce the necessary traction to pull them through the soil. Consequently these tractors are always overpowered. Vibrating digger blades have been shown to reduce draft dramatically, 70 percent in one reported test (Al-Jubori and McNulty, 1980[1]). The use of oscillating blades has been proposed by many researchers with the objectives of reducing potato damage and losses, reducing the power required to pull the harvester through the soil and improving the separation efficiency of potatoes from soil (Gunn and Tramontini,[2] 1955; Harrison,[3] 1973; Johnson,[4] 1974; Johnson and Buchele,[5] 1969; Saqib, et. al.,[8] 1982). The oscillation of soil-working parts on tillage implements reduces draft and permits the use of lighter tractors. Power not used for draft, because of traction limitations, is available through the tractor power take-off to oscillate soil-working parts of tillage implements.

II. DESIGN OF VIBRATORY DIGGER BLADE

A four-bar mechanism with an eccentric cam on each side of the digger blade was designed to produce given amplitudes. The power was transmitted to the driving shaft from the PTO of the tractor through a gearbox. At each end of the cam shaft identical cams were attached at identical angles of rotation to the two connecting rods which in turn were attached by floating hinge joints to the vibratory digger blade. The other ends of digger blade were hinged to the frame of

* 江原大學校 農科大學 農工學科

** Department of Agricultural Engineering, Louisiana State University

*** 서울大學校 農科大學 農工學科

the digger unit. The digger blade assembly is shown in Figure 1.

The dimensions of the four-bar mechanism are shown in Figure 2. The cam eccentricity, O_2-A, estabilished the maximum amplitude of the trailing edge of the digger blade bottom plate. This bottom plate was 622.3 mm wide and 441.3 mm long. Steel plate 9.5 mm thick was used to build the blade assembly and connecting rods. The center portion of the bottom plate was made of nineteen thin steel bars to improve the break-up and separation efficiency of the digger blade and to reduce its inertia. The side-view of the mechanism is shown in Figure 3.

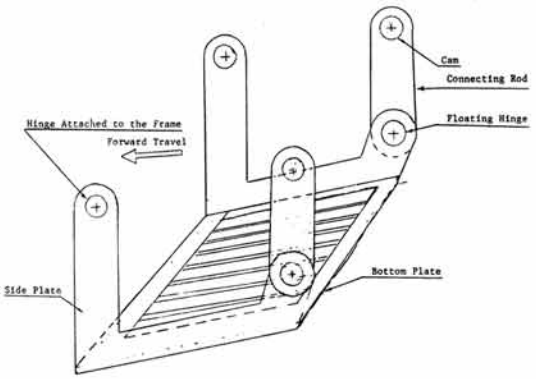

Figure 1. Side view of vibrating digger blade.

III. ACCELERATION ANALYSIS

A Kinematic analysis of the vibrating assembly was made to determine the accelerations of the various parts. These accelerations were then used to find the unbalanced forces. The analysis was based on the use of complex numbers (Mable and Ocvirk,[6] 1978; Shigley and Uicker,[7] 1980).

In Figure 4, a line connecting O_2 and O_4 was considered as the positive real axis, and a downward vertical line was selected as the positive imaginary axis. Counter-clockwise rotation of the cam (O_2-A) was regarded as the positive direction of rotation for the moving links.

r_e and θ_e as Functions of Known Variables :

From the vector triangle O_2O_4A

$$\vec{R}_1 = \vec{R}_2 + \vec{R}_e$$
$$\vec{R}_e = \vec{R}_1 - \vec{R}_2 \qquad (1)$$

Equation (1) expressed in the form of complex numbers is:

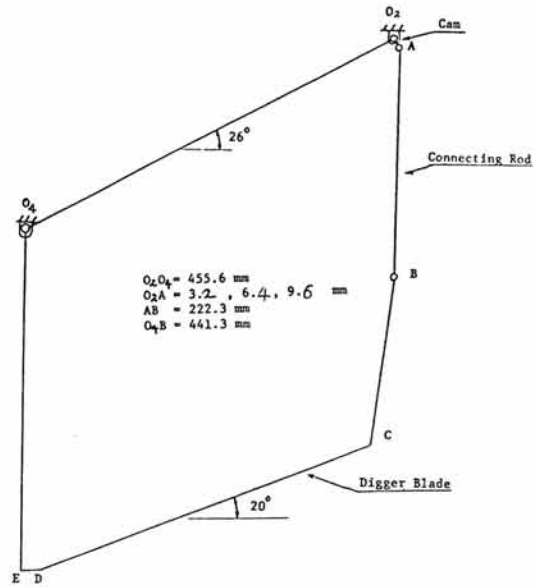

Figure 2. Kinematic representation and dimensions of digger blade.

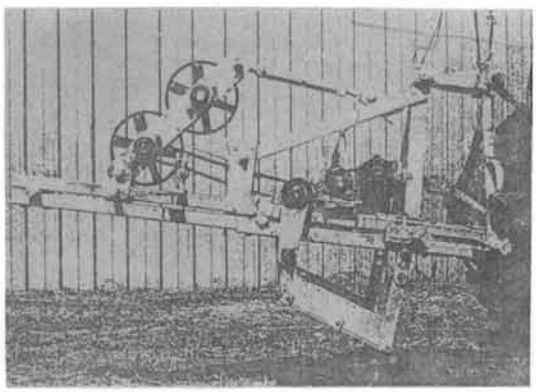

Figure 3. Side view of digger blade mechanism.

$$r_e e^{i\theta_e} = r_1 e^{i\theta_1} - r_2 e^{i\theta_2} \quad (\theta_1 = 0)$$

$$r_e(\cos\theta_e + i\sin\theta_e = r_1 - r_2 (\cos\theta_2 + i\sin\theta_2) \qquad (2)$$

O_4 $\vec{R_1}$ O_2 $\vec{R_2}$ θ_2 $\vec{R_e}$ $\vec{R_4}$ θ_4 $\vec{R_B}$ θ_2 A θ_e $\vec{R_3}$ B

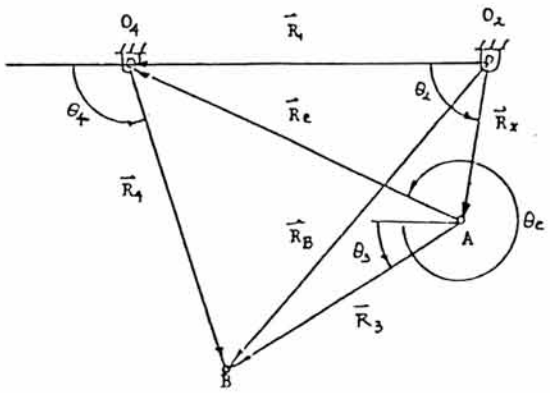

Figure 4. Position vectors of digger blade.

Equation (2) divided into real and imaginary components is:

$$\text{Real: } r_e\cos\theta_e = r_1 - r_2\cos\theta_2 \qquad (3)$$

$$\text{Imaginary: } r_e\sin\theta_e = -r_2\sin\theta_2 \qquad (4)$$

From equations (3) and (4)

$$r_e^2 = r_1^2 + r_2^2 - 2r_1r_2\cos\theta_2 \qquad (5)$$

$$\theta_e = \sin^{-1}\left(-\frac{r_2}{r_e}\sin\theta_2\right) \qquad (6)$$

Displacements

θ_3 and θ_4 as Functions of r_e and θ_e:

From vector triangle ABO_4

$$\vec{R_3} = \vec{R_e} + \vec{R_4}$$

$$= r_3 e^{i\theta_e} + r_4 e^{i\theta_4}$$

$$r_3(\cos\theta_3 + i\sin\theta_3) = r_e(\cos\theta_e + i\sin\theta_e) + r_4(\cos\theta_4 + i\sin\theta_4)$$

$$\text{Real: } r_3\cos\theta_3 = r_e\cos\theta_e + r_4\cos\theta_4 \qquad (7)$$

$$\text{Imaginary: } r_3\sin\theta_3 = r_e\sin\theta_e + r_4\sin\theta_4 \qquad (8)$$

From equations (7) and (8)

$$r_3^2 = r_e^2 + r_4^2 + 2r_er_4\cos\theta_e\cos\theta_4 + 2r_er_4\sin\theta_e\sin\theta_4 = r_e^2 + r_4^2 + 2r_er_4\cos(\theta_e - \theta_4)$$

$$\cos(\theta_e - \theta_4) = \frac{r_3^2 - r_e^2 - r_4^2}{2r_er_4}$$

$$\theta_4 = \theta_e \div \cos^{-1}\left[\frac{r_3^2 - r_e^2 - r_4^2}{2r_er_4}\right] \qquad (9)$$

From equations (7) and (8)

$$r_4\cos\theta_4 = r_3\cos\theta_3 - r_e\cos\theta_e \qquad (10)$$

$$r_4\sin\theta_4 = r_3\sin\theta_3 - r_e\sin\theta_e \qquad (11)$$

From equations (10) and (11)

$$r_4^2 = r_3^2 + r_e^2 - 2r_3r_e(\cos\theta_3\cos\theta_e + \sin\theta_3\sin\theta_e)$$

$$\theta_3 = \theta_e + \cos^{-1}\left[\frac{r_3^2 + r_e^2 - r_4^2}{2r_3r_e}\right] \qquad (12)$$

Velocities

ω_3 and ω_4 as Functions of θ_3 and θ_4 :

From vector triangles ABO_2 and BO_4O_2

$$\vec{R_B} = \vec{R_2} + \vec{R_3} = \vec{R_1} + \vec{R_4} \qquad (13)$$

Differentiating equation (13) with respect to time t would yield velocity of point B.

$$V_B = \frac{dR_B}{dt} = \frac{d(r_2 e^{i\theta 2})}{dt} + \frac{d(r_3 e^{i\theta 3})}{dt}$$

$$= \frac{d(r_1 e^{i\theta 1})}{dt} + \frac{d(r_4 e^{i\theta 4})}{dt} \quad \text{where } \theta_1 = 0$$

$$r_2\omega_2 (ie^{i\theta 2}) + r_3\omega_3 (ie^{i\theta 3}) = r_4\omega_4 (ie^{i\theta 4}) \quad (14)$$

Expanding the equation (14)

$$r_2\omega_2 (ics\theta_2 - \sin\theta_2) + r_3\omega_3 (i\cos\theta_3 - \sin\theta_3) = r_4\omega_4 (i\cos\theta_4 - \sin\theta_4)$$

Real: $r_2\omega_2\sin\theta_2 + r_3\omega_3\sin\theta_3 = r_4\omega_4\sin\theta_4$ (15)

Imaginary: $r_2\omega_2\sin\theta_2 + r_3\omega_3\cos\theta_3 = r_4\omega_4\cos\theta_4$ (16)

Equations (15) and (16) could be expressed in matrix form

$$\begin{bmatrix} -r_3\sin\theta_3 & r_4\sin\theta_4 & \omega_3 \\ -r_3\cos\theta_3 & r_4\cos\theta_4 & \omega_4 \end{bmatrix} = \begin{bmatrix} r_2\omega_2\sin\theta_2 \\ r_2\omega_2\cos\theta_2 \end{bmatrix}$$

$$\omega_3 = \frac{r_2\omega_2\sin\theta_2\, r_4\cos\theta_4 - r_4\sin\theta_4\, r_2\omega_2\cos\theta_2}{-r_3 r_4\sin\theta_3\cos\theta_4 + r_3 r_4\sin\theta_4\cos\theta_3}$$

$$= \frac{r_2 r_4\omega_2\sin(\theta_2 - \theta_4)}{r_3 r_4\sin(\theta_4 - \theta_3)} = \frac{r_2\omega_2\sin(\theta_2 - \theta_4)}{r_3\sin(\theta_4 - \theta_3)} \quad (18)$$

$$\omega_4 = \frac{-r_3\sin\theta_3\, r_2\omega_2\cos\theta_2 + r_3\cos\theta_3 r_2 w_2\sin\theta_2}{r_3 r_4\sin(\theta_4 - \theta_3)}$$

$$= \frac{r_2\omega_2\sin(\theta_2 - \theta_3)}{r_4\sin(\theta_4 - \theta_3)} \quad (19)$$

Accelerations

α_3 and α_4 as Functions of ω_3 and ω_4 :

Differentiating equation 1(14) with respect to time t

$$ir_2 (\alpha_2 e^{i\theta 2} + i\omega_2^2 e^{i\theta 2}) + ir_3 (\alpha_3 e^{i\theta 3} + i\omega_2^2 e^{i\theta 3}) = ir_4 (\alpha_4 e^{i\theta 4} + i\omega_4^2 e^{i\theta 4})$$

$$r_2(i\alpha_2 - \omega_2^2) e^{i\theta 2} + r_2 (i\alpha_3 - \omega_3^2) e^{i\theta 3} = r_4(i\alpha_4 - \omega_3^2) e^{i\theta 4}$$

$$r_2 (i\alpha_2 - \omega_2^2)(\cos\theta_2 + i\sin\theta_2) + r_3(i\alpha_3 - \omega_3^2)(\cos\theta_3 + i\sin\theta_3) = r_4(i\alpha_4 - \omega_4^2)(\cos\theta_4 + i\sin\theta_4)$$

Real: $r_2(\alpha_2\sin\theta_2 + \omega_2^2\cos\theta_2) + r_3(\alpha_3\sin\theta_3 + \omega_3^2\cos\theta_3) = r_4(\alpha_4\sin\theta_4 + \omega_4^2\cos\theta_4)$

Imaginary : $r_2(\alpha_2\cos\theta_2 - \omega_2^2\sin\theta_2) + r_3(\alpha_3\cos\theta_3 - \omega_3^2\sin\theta_3) = r_3(\alpha_4\cos\theta_4 - \omega_4^2\sin\theta_4)$

$$\begin{bmatrix} -r_3\sin\theta_3 \cdot r_4\sin\theta_4 \\ -r_3\cos\theta_3 \cdot r_4\cos\theta_4 \end{bmatrix} \begin{bmatrix} \alpha_3 \\ \alpha_4 \end{bmatrix} = \begin{bmatrix} r_2(\alpha_2\sin\theta_2 + \omega_2^2\cos\theta_2) + r_3\omega_3^2\cos\theta_3 - r_4\omega_4^2\cos\theta_4 \\ r_2(\alpha_2\cos\theta_2 - \omega_2^2\sin\theta_2) - r_3\omega_3^2\sin\theta_3 + r_4\omega_4^2\sin\theta_4 \end{bmatrix} \quad (20)$$

where $\alpha_2 = 0$

Solving equation (20)

$$\alpha_3 = [r_2\omega_2^2\cos(\theta_4 - \theta_2) + r_3\omega_3^2\cos(\theta_4 - \theta_3) - r_4\omega_4^2]/r_3\sin(\theta_4 - \theta_3) \quad (21)$$

$$\alpha_4 = -r_2\omega_2^2\cos(\theta_3 - \theta_2) + r_4\omega_4^2\cos(\theta_3 - \theta_4) - r_3\omega_3^2 \Big/ r_4\sin(\theta_3 - \theta_4) \quad (22)$$

Equations (5), (6), (9), (12), (18), (19), (21), and (22) were input to a computer program and the accelerations of the connecting links and digger blade assembly were obtained for every five degrees of cam rotation at a given cam rotational velocity of 1542 rpm.

IV. FORCE ANALYSIS

The centers of gravity of the connecting rod and digger blade assembly were determined by dividing them into several tiangles and parallelograms, and by finding the area and centers of gravity of each geometry and taking moments from a given point. The total mass of the digger blade was 18.1 kg and that of the connecting rods 8.9 kg.

Determination of the Unbalanced Forces

The mass ratio of the digger blade assembly to the connecting rod was:

$$M_b / M_c = 18.1 / 8.9 \cong 2$$

To determine the maximum unblanced forces for the connecting rod and the digger blade assembly the maximum accelerations of each component for the greatest amplitude level used, 9.6 mm, was calculated. These are listed in Table 1 at the angular displacement of the driving cam at which they occured, 70 degrees. The angular velocity of the cam was 1542 rpm. The acceleration of the center of gravity of connecting rod was approximaterly 0.79 times of that of the blade assembly. The unbalanced force due to the eccentricity of the cam was neglected because the eccentricity and mass of the cams were very small.

Table 1. Accelerations of the Centers of gravity of connecting rod and digger blade assembly at cam angle, 70 degrees.

Amplitude (mm)	Connecting Rod (m/s^2)	Digger Blade Assembly (m/s^2)
9.6	132.33	171.92

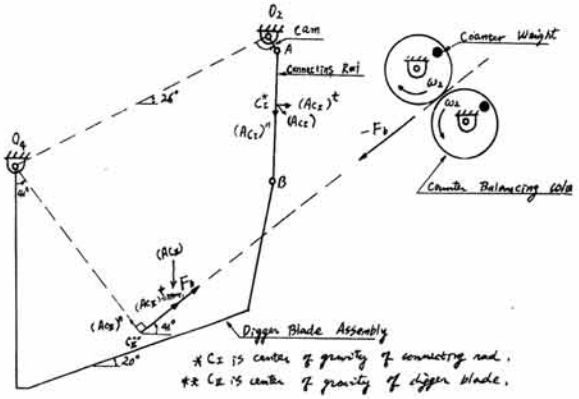

Figure 5. Acceleration vectors of the connecting rod and digger blade assembly.

There were two major unbalanced forces, one was developed by the connecting rod and the other by the digger blade assembly. Considering the effects of acceleration on the total unbalanced force of the whole system that of the digger blade assembly was dominant because unbalanced force F_b of the blade assembly was M_b (Ac11) and that F_c of connecting rod was M_c(Ac1) = (M_b/2) (0.79) (Ac1) = 0.40 F_b. To design a mechanically

balanced vibratory digger blade both major unbalanced forces should be balanced. Because the unbalanced force produced by the digger blade assembly was the greater one and because of the limitation of space and the complexity in designing the counter balancing mechanism, a counter balancing force was applied for the cam angular displacement of 70 degrees. The direction of unbalanced force acting on the whole system was approximately 41 degrees clockwise from horizontal plane (Figure 5).

V. COUNTER BALANCING

To counterbalance the unbalanced force F_b two identical counter-rotating gears were used (Figure 5). Their angular velocities were the same as that of the cam. The direction of the balancing force developed by the counter-balance weights attached on two gears was opposite to F_b and of equal magnitude. The calculations to determine the weight of the counter weights were based on the centrifugal force developed at a constant angular velocity of 1542 rpm.

Table 2 summarizes the counter balancing analysis. Figure 6 shows the unbalanced and counterweight forces in polar coordinates for a complete cam cycle of 360 degrees. As shown in Figure 6, most part of the unbalanced force generated by the blade assembly was canceled by the counter-balancing mechanism applied to this study.

Table 2. Summary of counter balancing.

Amplitude of Vibration	Angle*	Counter Weight for Each Gear	Radius to Weight
9.6 mm	41°	6.25N	95.3mm

*Angle of balanced force, counter-clockwise from the horizontal plane.

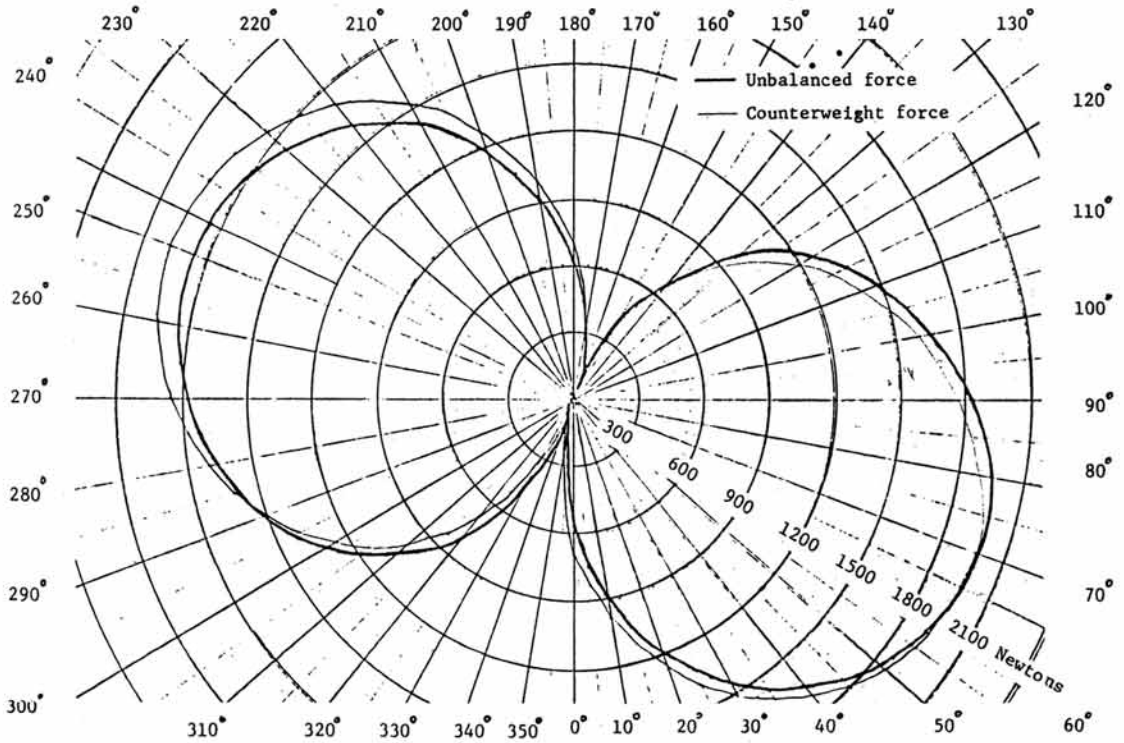

Figure 6. Unbalanced and counterweight force for a complete cam cycle of 360 degrees.

VI. TORQUE ANALYSIS

The torque on the input shaft was divided into four components. These were the torque due to (1) the motion of the connecting rod, (2) the motion of the blade assembly, (3) the weight of the blade assembly and connecting rod, and (4) the friction (mabie and Ocvirk[6]1978; Shigley and Uicker[7]1980). The general representation of force and torque acting on a four-bar linkage is shown in Figure 7. Following is a list of the parameters depicted.

M_3 : Mass of connecting rod, 8.9 kg
M_4 : Mass of digger blade, 18.1 kg
I_3 : 0.02311 kg.m^2
I_4 : 0.59212 kg.m^2
ω_2 : Angular speed of cam
α_4 : Angular acceleration of the digger blade
T_2 , T_4 : Torques acting on the cam and digger blade
r_3 : Location of center of mass of connecting rod
Fo_3 : Inertia force of connecting rod
Ag_3 : Total acceleration of mass center of connecting rod
f_3 : Offset from Ag_3
ℓ_3 : Location of line of action of Fo_3

The mass moment of inertia I_3 and I_4 for the connecting rod (link 3) and blade assembly (link 4) were measured by using the principle of compound pendulum. The theretical total torque, T, of the system consisted of the torque due to the connecting rod, Ts, the torque due to the blade assembly, T_2, and the torque due to the weight of the components, T_{stat}. Friction in the drive mechanism also created additional torque.

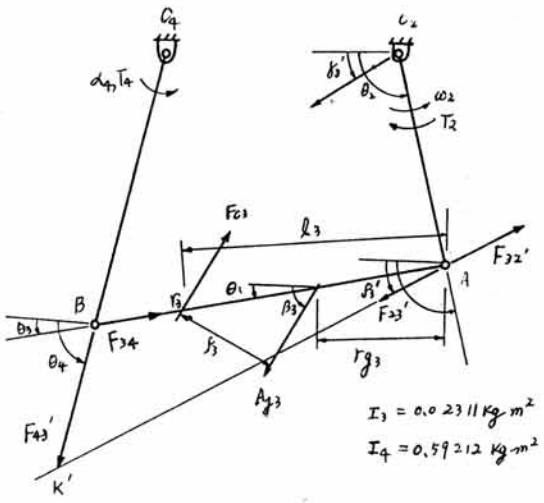

Figure 7. A four-bar linkage with T_4 and Fo_3 acting.

Torque due to the inertial force, Fo_3, of the connecting rod:

From Figure 7:

$$Fo_3 = M_3 Ag_3 e^{i(\beta_3 + \pi)}$$

where $\beta_3 \tan^{-1}\left(\frac{Ag_3 Y}{Ag_3 X}\right)$

$$f_3 = I_3\alpha_3 / Fo_3$$

$$\ell_3 = rg_3 + \frac{f_3}{\sin(\beta_3 - \theta_3)}$$

$$\Sigma M_A = 0$$

$$F_{43}' r_3 \sin(\theta_4 - \theta_3) - Fo_3 \ell_3 \sin(\beta_3 - \theta_3) = 0$$

$$F_{43}' = \frac{Fo_3 \ell_3 \sin(\beta_3 - \theta_3)}{r_3 \sin(\theta_4 - \theta_3)}$$

$$F_{23}' + F_{43}' + Fo_3 = 0$$

$$F_{23}' e^{i\gamma_3'} + F_{43}' e^{i\theta_4} + Fo_3 e^{i(\beta_3 + \pi)} = 0$$

Real: $F_{23}'\cos\gamma_3' + F_{43}'\cos\theta_4 + Fo_3\cos(\beta_3 + \pi) = 0$

Imaginary: $F_{23}'\sin\theta_3' + F_{43}'\sin\theta_4 + Fo_3'\sin(\beta_3 + \pi) = 0$

Real and imaginary components of F_{23}'

$$\Re F_{23}' = F_{23}\cos\gamma_3' = -F_{43}'\cos\theta_4 - F_{03}\cos(\beta_3 + \pi)$$

$$\varphi F_{23}' = F_{23}\sin\gamma_3' = -F_{43}'\sin\theta_4 - F_{03}\sin(\beta_3 + \pi)$$

$$F_{23}' = \sqrt{(\Re F_{23}')^2 + (\varphi F_{23}')^2}$$

$$\gamma_3' = \mathrm{Tan}^{-1}\left(\frac{\varphi F_{23}'}{\Re F_{23}'}\right)$$

$$\therefore T_s = -F_{32}'r_2\sin(\theta_2 - \gamma_3')$$

This torque is shown in Figure 8 for one cycle of driving link 2 at a rotational velocity of 1542 rpm with no load on the digger blade.

Torque, T_2, due to the blade assembly:

From Figure 7

$$I_4\alpha_4 = T_4 = r_4F_{34}\mathrm{Sin}\gamma = r_4F_{34}\mathrm{Sin}(\theta_4 - \theta_3)$$

$$F_{34} = \frac{I_4\alpha_4}{r_4\mathrm{Sin}(\theta_4 - \theta_3)}$$

$$T_2 = r_2F_{34}\mathrm{Sin}(\theta_2 - \theta_3) = \frac{r_2T_4\mathrm{Sin}(\theta_2 - \theta_3)}{r_4\mathrm{Sin}(\theta_4 - \theta_3)}$$

The torque T_2 due to T_4 was ploted in Figure 8 with the driving cam speed of 1542 rpm.

Torque, T_{stat}, Due to the Weight of Blade Assembly and Connecting Rod:

In Figure 9 approximate reaction, R_{cam}, at the driving cam (link 2) could be obtained by calculating the reaction at B because the length of link 2 was small compared with the other dimensions.

Reaction R_{cam} on the cam

$$R_{cam} = W_{Rod} + W_{Blade} \times \frac{\ell_1}{L}$$

$$= 87.3 + 177.6 \times \frac{190.5}{431.8} = 165.7$$

Newtons

Torque, T_{stat}, due to the weight of the blade and rod

$$T_{stat} = R_{cam} \times R_2\mathrm{Cos}(\theta_2 + 26)$$

where R_2 was the eccentricity of the cam. T_{stat} was shown in Figure 7 for one cycle of driving cam. Theoretical torque T_{th}

$$T_{th} = T_s + T_2 + T_{stat}$$

is shown in Figure 8.

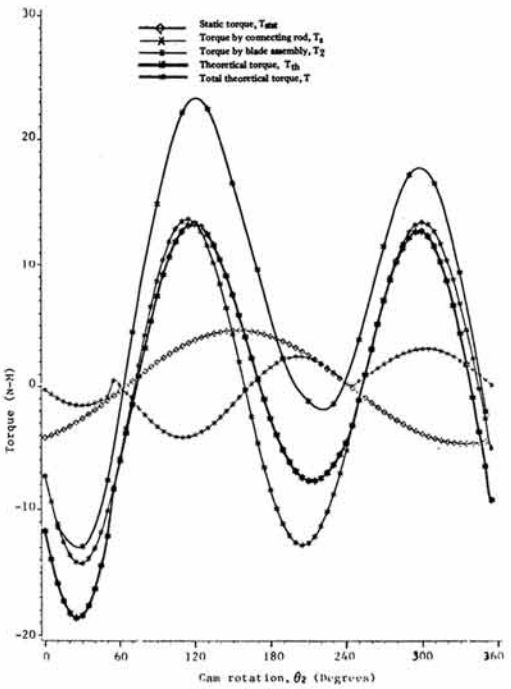

Figure 8. Torque curves generated by each component.

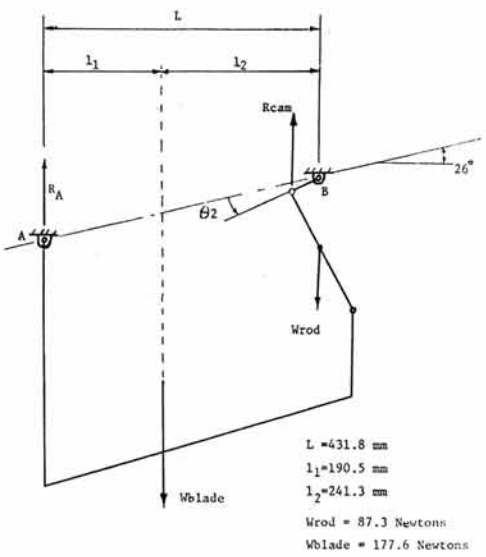

Figure 9. Reaction at the driving shaft due to the weight of the connecting rod and digger blade assembly.

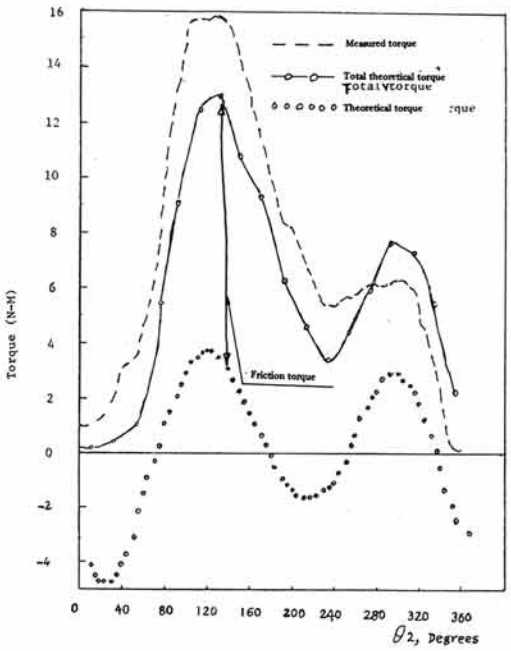

Figure 10. Measured torque, friction torque, theoretical total torque, and theoretical torque with the cam speed of 768 rpm and with no load.

Friction Torque:

The friction torque in the drive system between the torque transducer and the cams was measured in the laboratory at 20 degrees intervals for a complete revolution of the cam shaft. This torque was added to the theretical torque to give the theretical total toque, T, when the vibrating blade was operated. Torque due to the cams could not be measured without introducing the inertial force of the connecting rods.

Laboratory Tests:

A Himmelstein torque transducer and amplifier was included in the drive for the camshaft. This unit was carefully calibrated by applying pure torque loads to the cam shaft. Dynamic torque output from the torque transducer and amplifier was compared to the theoretical total torque which is sum of theoretical torque and friction torque (Figure 10). These tests were made with the mechanism driven at 768 rpm, the maximum speed at which the device could be tested in the laboratory. The difference between the theortical and measured torque was believed to be due to: (1) the cam friction, (2) the additional frictional load due to dynamic forces (not measured during the static calibration procedures), and the torque to drive the balancing mechanism which was not included in the theoretical torque analysis.

VII. CONCLUSIONS

1. The major portion of the unbalanced forces produced by the oscillation of the

digger blade were canceled by the counter balancing force generated by the balancing mechanism which is composed of two counter-rotating gears.

2. The difference between the theoretical nd measured torque was believed to be due to dynamic frictional loads which was not measured during the static calibration procedures and the torque to drive the balancing mechanism which was not included in the theoretical torque analysis.

REFERENCES

1. Al-Jubouri, K. and P.B. McNulty. 1980. Vibratory potato digging. Proc. of the 5th Int. Con. on the Mech. of Field Energy (IAMFE). Wageningen, Netherlands, pp. 264-268.
2. Gunn, J.T. and V.N. Tramontini. 1955. Oscillation of tillage implements. Agri. Eng., 36(11): 725-729.
3. Harrison, H.P. 1973. Draft, torque, and power requirements of a simple vibratory tillage tool. Canadian Agric. Eng., 15(2): 71-74.
4. Johnson, L.F. 1974. A vibrating blade for the potato harvester. Trans. of the ASAE, 17(5): 867-870, 873.
5. Johnson, C.E. and W.F. Buchele. 1969. Energy in clod-size reduction of vibratory tillage. Trans. of the ASAE, 12(3): 371-374.
6. Mabie, H.H. and F.W. Ocvirk. 1978. Mechanisms and dynamics of machinery. J. Willey and Sons. pp. 361-364, 428-434.
7. Shigley, J.E. and J.J. Uicker. 1980. Theory of machines and mechanisms. McGraw-Hill. pp. 148-151, 484-490.
8. Saqib, G.S., M.E. Wright, and T.R. Way. 1982. Clod size reduction by viratory diggers. ASAE Paper No. 82-1546, St. Joseph, MI.

祝

學 位 取 得

姓　　名：李 英 烈
生 年 月 日：1934年 2月 28日生
勤 務 處：農村振興廳 農業機械化硏究所
取得學位名：農學博士
學位授與大學：圓光大學校
學位取得年月日：1986年 8月 26日
學 位 論 文：논耕耘方法別 所要에너지와 벼 收量에 關한 硏究